Available online at www.sciencedirect.com
SCIENCE DIRECT®
PERGAMON
International Journal of Heat and Mass Transfer 46 (2003) 3279–3289
International Journal of HEAT and MASS TRANSFER
www.elsevier.com/locate/ijhmt

Dynamics of filtration combustion front perturbation in the tubular porous media burner

K.V. Dobrego [a,*], I.M. Kozlov [a], V.I. Bubnovich [b], C.E. Rosas [b]

[a] *Luikov's Heat and Mass Transfer Institute, Chemical Physics Laboratory, National Academy of Sciences of Belarus, 15 P. Brovki Street, Minsk 220072, Belarus*

[b] *Department of Mechanical Engineering, University Santiago de Chile, B.O'Higgins 3363, Casilla 10233, Santiago, Chile*

Received 20 December 2002

Abstract

The state-of-the-art of filtration combustion instability researches is presented. Dynamics of filtration combustion inclination instability is investigated experimentally, analytically and numerically. It is found that inclination amplitude growth velocity on the linear stage is proportional to filtration combustion wave velocity u_w, system diameter D_0 and inversed diameter of porous media particles d_0 : $\Delta\dot{X} \sim u_w(D_0/d_0)$.

The tendency of thermal compensation of perturbation is confirmed by experiments and 2D numerical simulation. In the case of inclination growth stoppage, inclination maximum amplitude or amplitude of saturation can be estimated via the dimensionless wave velocity u and system geometrical parameters $\Delta X_{max} \sim (u/(1-u))(D_0^2/d_0)$.

The concept of perturbation two-staged evolution, which includes initial linear perturbation growth due to local filtration redistribution and following complex thermal and hydrodynamic reorganization of the system, is supported by experimental data and 2D simulation.

© 2003 Elsevier Science Ltd. All rights reserved.

1. Introduction

Gas filtration combustion (FC) or combustion in an inert porous media is utilized in numerous technical applications such as VOCs oxidation, lean combustible mixtures burning under superadiabatic (excess enthalpy) condition, catalyst treatment by thermal wave, as well as for organization of various thermochemical processes [1,2].

FC wave front can be unstable, i.e. not preserve its startup geometry, which is a basic obstacle to widely use the FC devices in industry. From the physical viewpoint, the instability is a non-steady growth of FC front perturbation, which leads to combustion extinguishing or to emergence of new (stable) front structure. The inclination and hot-spot instability were distinguished in experiments [3,4]. Vainstein [5] considered thermal and hydrodynamic instability problems independently. One-dimensional thermal perturbations were under investigation. A conclusion of absolute stability of FC front to heat perturbations in a wide range of parameters follows from [5]. Analysis of hydrodynamic instability in [5] considered 2D problem. As shown, provided that filtration coefficients do not differ strongly on both sides of combustion front, the flame is hydrodynamically unstable.

Minaev and colleagues [4] studied FC stability problem experimentally and theoretically. Inclination instability of the front was observed in a quartz tube of 40 mm diameter at downstream FC regimes. Unfortunately, the work does not contain any information on the peculiarities of inclination dynamics, front break conditions, etc. The problem was considered analytically for long-wave (considerably exceeding front width) perturbations. A case of short-wave perturbations was also considered by means of parameterization of the front local velocity via front curvature f'' (Markstein's method) $u_w = u_{w,0}(1 + \gamma f'')$, ($\gamma$—positive constant). As a result of above assumption and the fact that the model

* Corresponding author. Tel.: +375-17-284-2021; fax: +375-17-284-2212.

E-mail address: kdob@itmo.by (K.V. Dobrego).

0017-9310/03/$ - see front matter © 2003 Elsevier Science Ltd. All rights reserved.
doi:10.1016/S0017-9310(03)00125-X

Nomenclature

c	heat capacity
D_0	burner tube diameter or perturbation transverse size
d_0	diameter of particle of porous bed
f''	front local curvature
G	gas mass flow rate
H	gasdynamic clog (hot zone) width in the porous body
h	perturbation amplitude (cavity mean depth)
h_i	specific enthalpy of ith component
k	filtration permeability
l_{th}	length of thermal relaxation
l_{hd}	hydrodynamic relaxation length
L	total length of porous body
p_{o}	pressure at the outlet of burner
Δp	pressure drop in burner
Δp_{cold}	pressure drop in the cold (not operating) burner
p_{l}	mean pressure in the coordinate of the front
$\tilde{q}$	specific heat flux to the preheating zone of unperturbed front
Q_λ	heat flux to the preheating zone mean over perturbation cross-section
$T_{\max}$	maximum temperature in the filtration combustion wave front
T_0	initial or ambient temperature
$u_{\text{w}}, u_{\text{w},0}$	flame front velocity and unperturbed flame front velocity
u_{t}	thermal wave velocity in porous media
$u = u_{\text{w}}/u_{\text{t}}$	dimensionless wave front velocity
u_{g}	gas filtration velocity
x	coordinate along the axis of the burner

Greek symbols

β	coefficient of Newtonian heat losses of the burner, W/(m^3 K)
λ	thermal conductivity of porous bed
Δ	variation or difference
ε^*	emissivity
$\delta_{\text{P}}, \delta_{\text{T}}$	initial perturbation amplitude parameters
ΔX	inclination amplitude (difference between "head" and "tail" of front coordinates)
$\Delta \dot{X}$	time derivative of inclination amplitude
μ	gas viscosity
ρ	density
σ	Stephan–Boltzmann constant
τ_{comp}	perturbation compensation time
$\phi = \tilde{q}_\lambda/\tilde{q}_{\text{u}}$	dimensionless factor

Subscripts

cr	critical value
ch	characteristic value
g	gas
s	solid
λ	having conductive nature
u	having convective nature

indirectly (via boundary conditions) consider peculiarities of the thermal problem, the authors obtained a formula for perturbation critical size, practical use of which is straightened because of undefined γ.

The problem of FC front thermal instability for small 2D perturbations of the front in approximation of instantaneous reaction is considered in [7]. Reaction rate variation with temperature was considered by Frank–Kamenetsky expansion of Arrhenius function. Perturbation amplification factor is determined and critical perturbation wavelength is defined. It is shown that higher growth rate corresponds to longer wavelength perturbations.

The experience of the works [3–7] let one conclude that satisfactory theory of FC wave instability should take into account interrelation of hydrodynamic (perturbation of filtration field) and thermal factors, regard multi-dimension of the perturbations, and consider not only local front characteristics, but system macroscopic parameters.

A certain progress in investigation of FC instability problem has been made recently [8–12]. New methods to analyze the stability, namely, the method of flow competition (MFC) to analyze dynamic behavior of perturbations [8] was proposed, filtration problem small perturbation (SP) analysis [9] was performed. The said methods let one to obtain estimates for front instability criterion and describe some qualitative peculiarities of wave front dynamics. It was shown that SPs may be restrained at low level or get an limited growth depending on system parameters, main of which is hydrodynamic clog width to system diameter ratio. The data of experimental investigation of front inclination presented in [12], gave grounds for more profound analysis of inclination perturbation at linear and following non-linear phase. According to [12] the local and linear models deliver the necessary conditions for perturbation growth. The non-linear stage is characterized with complex reorganization of thermal and filtration fields that tend to compensate perturbation. It is proposed to characterize perturbation evolution on non-linear stage with characteristic times of perturbation growth and system compensation of the perturbation. The adequacy of this concept to experimental data was

discussed. The works [8–12] include models and concepts for qualitative analysis of stability of FC systems. Experimental investigation of the problem is complicated task due to stochastic nature of the porous media, filtration flow and bad reproducibility of measurements. The numerical simulation of realistic FC systems in these conditions should become important element of investigation.

In this article a short presentation of named concepts and methods is given. Experimental data on inclination instability in the tubular reactor at elevate pressure are presented and their conformity to the theoretical model is discussed. The results of 2D numerical simulation of FC perturbation dynamics are presented. The model of FC perturbation is tuned with regard to the simulation results.

2. Qualitative theory of thermal-hydrodynamic instability of filtration combustion front

According to the models [8–10] the joint and interrelated effect of thermal field change and filtration redistribution over the cross-section is responsible for front perturbation evolution. Physically perturbation amplification is caused by filtration field redistribution near the flame front in such a way that the total gas flow rate in the perturbation cross-section grows with the perturbation amplitude increase. At the same time competing process of conductive and radiative heat transfer compensates perturbation growth. To consider interaction of the thermal and hydrodynamic factors the MFC was proposed in [8]. According to this method the heat balance of combustion front preheating zone in the cross-section of front perturbation, Fig. 1, is evaluated. Assuming the temperature of the front is constant independently of perturbation and using simple models for evaluation of the conductive $Q_\lambda(h)$ and convective $Q_u(h)$ heat fluxes as a function of the perturbation amplitude h [8,10] one can analyze perturbation dynamics.

According to MFC a SP grows if convective flux accretion caused by the perturbation exceeds the competing growth of the conductive flux,

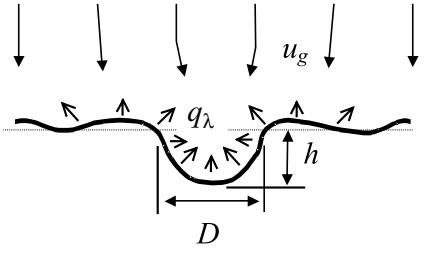

Fig. 1. Schematics of perturbation cavity and thermal and convection fluxes redistribution.

$$\delta Q_u(h) > \delta Q_\lambda(h) \tag{1}$$

By using simple geometrical model for perturbation cavity one can obtain and analyze the conditions for the inequity (1). The correspondent inequity

$$\frac{4h}{D_0}\tilde{q}_\lambda < \frac{D_0}{2(H-h)}\tilde{q}_u + \frac{2}{3}\frac{h^2}{(H-h)D_0}\tilde{q}_u. \tag{2}$$

was analyzed in [8]. Here $\tilde{q}_\lambda$, $\tilde{q}_u$ are specific conductive and convective fluxes for unperturbed front, h—perturbation cavity mean depth, D_0—its transverse size, H—width of gasdynamic clog (hot zone) in the porous body. Analysis of quadratic relative to h inequality (2) shows that shallow perturbations $(h \ll D_0, h \ll H)$ always grow. Depending on Eq. (2) discriminant perturbation growth can either stop at certain characteristic amplitude $h = h_{ch}$

$$h_{ch} = \frac{3H\phi}{1+6\phi}\left(1 - \sqrt{1 - \frac{D_0^2}{H^2}\frac{(1+6\phi)}{12\phi^2}}\right) \tag{3}$$

or continue to grow permanently (here notation $\phi = \tilde{q}_\lambda/\tilde{q}_u$ is used). In amplitude interval $h_{ch} < h < h_{cr}$ perturbations cannot grow and fall to h_{ch}. Condition of absolute front instability for the considered geometrical class of perturbations follows from discriminant negativity of (2).

The important parameter of the MFC model is the width of gasdynamic clog H. It can be expressed by easily measurable values—total length of porous body L, pressure drop in the cold Δp_{cold} and hot Δp (operating) systems at same gas flow rate and maximal temperature in the wave front T_{max} [10].

$$H = L\frac{\Delta p/\Delta p_{cold} - 1}{(T_{max}/T_0)^{3/2} - 1}. \tag{4}$$

In the work [10] SP analysis for FC front amplification was performed by using Darsi–Leibenzon filtration equation. The SP analysis let one estimate perturbation growth increment Ω [s^{-1}] on the initial (linear) stage. According to [10] in the long wave limit (perturbation dimension is much higher than flame front width) $\Omega \sim (\partial u_w/\partial u_g)u_g$. By using definition of dimensionless wave velocity $u \equiv u_w/u_t$ and thermal wave velocity $u_t \equiv (c\rho_g/c\rho_s)u_g$ this estimation may be rearranged in form $\Omega \sim (u_w + u_t u_g \partial u/\partial u_g)$. As far as function $u(u_g)$ comes to saturation [8], $\partial u/\partial u_g \to 0$ for sufficiently big filtration rates

$$\Omega \sim u_w. \tag{5}$$

Taking into account the final dimensions of perturbation (short wave limit) leads to conclusion of critical perturbation size existence. The value of the perturbation time increment Ω becomes in this case non-linear function of perturbation diameter. The characteristic value of Ω in the same degree of accuracy as (5) can be expressed as

$$\Omega \cong \frac{u_g^2(\partial u_w/\partial u_g)^2}{8\gamma u_t} \approx \frac{u_w u}{8\gamma} \approx \frac{1}{16}\frac{u_w}{d_0}. \quad (6)$$

Here the estimate $\gamma \approx 2d_0 u$ obtained for short wave perturbation limit [8] was used.

According to [7] perturbation growth increment is proportional to the perturbation wavelength. The wavelength of inclination perturbation may be associated with maximum transverse size—diameter of the combustor and using (6) one comes to correlation for inclination perturbation growth rate:

$$\frac{\Delta\dot{X}}{D_0} \sim \frac{u_w}{d_0}. \quad (7)$$

Here ΔX—coordinates difference between the head and tail of inclined FC front, Fig. 2.

The models described above consider perturbation smallness, use mainly local parameters of the system and will be referred to as local or linear models. All these models predict existence of characteristic perturbation amplitudes (background perturbation amplitude which cannot be eliminated), critical perturbation amplitudes (exceeding of which leads to unlimited perturbation growth) and absolute instability condition (criterion for perturbation unlimited growth). MFC model predicts small characteristic inclination $\Delta X_{ch}/D_0 \sim 1/4$ (at least for slowly propagating waves $u \leqslant 0.1$) and its inverse dependence on H. Instability criterion is expressed as hot zone width smallness condition according to all models. The critical hot zone width is close to unity $H_{cr}/D_0 \sim 1$ in the case of $u \sim 0.1$–0.4.

Experimental measurements of the front inclination dynamics performed in [12] confirmed existence of linear amplitude growth stage and effect of inclination saturation, which was first interpreted as characteristic perturbation amplitude ΔX_{ch}, described by the local models. At the same time experiments showed certain contradictions with the results of the local models: (1) in some cases inclination grew when instability criterion was not fulfilled, (2) the amplitude of front stabilization reached $\Delta X/D_0 = 1.5$–2 and noticeably exceeded estimates for characteristic inclination, predicted by the local models; (3) inclination of stabilization directly correlated with dimensionless wave velocity u and was independent of hot zone width. To explain these peculiarities it was supposed that local models correspond only to initial linear stage of the perturbation evolution [12] and at the later stage perturbation is controlled by system global scale thermal and hydrodynamic reorganization. The instability criteria implied by local models should be considered as *primary* (necessary) instability condition.

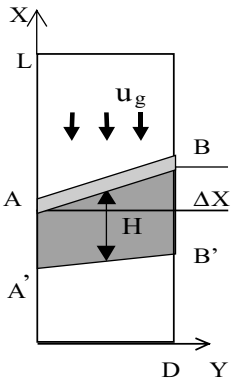

Fig. 2. Filtration combustion front inclination scheme. H—hot zone width, AB—wave front, A′B′—wave rear. Half-shaded area—front preheating zone.

Due to complexity of the thermo-hydrodynamic processes physically strict analysis of the non-linear stage of perturbation evolution is impossible. Nevertheless it is possible to distinguish main processes controlling thermal reorganization of the system. Relative movement of front sections in the process of inclination causes local temperature differentiation of these sections in accordance with local heat balance (higher velocity corresponds to higher T_{max}). In the case of negligible relative movement of the front sections the non-uniform filtration field ensure non-uniform enthalpy flux and causes gradual temperature growth in the part of the front where filtration velocity is higher (A point area in the Fig. 2). At the same time heat transfer along x axis increases, high temperature zone elongates which provides additional hydraulic resistance to filtration flux in the given cross-section.

At the later stage of perturbation evolution of front inclination reaches considerable amplitude the heat exchange interface surface increases and additional heat losses of the system result in reduced homogeneity and stability of front, particularly may lead to flame thermal quenching.

The named factors tend to compensate FC front perturbation and filtration field asymmetry (at least if perturbation did not change heat balance of the system considerably). This gives base for concept of two stages of front perturbation evolution: initial linear stage determined by local and unperturbed parameters of the front and following non-linear stage controlled by thermal and hydrodynamic reorganization of the system in whole. From this viewpoint instability of the practical FC systems is explained by final time of system thermal reorganization. In the hypothetic non-inertial porous media (small heat capacity) quick and complete compensation will secure stability of the front geometry even if primary instability condition [12] takes place.

Inclination dynamics on the non-linear stage is determined by intensity of perturbation compensation. The intensity can be characterized by characteristic time of the thermal reorganization process τ_{comp}. Following

this concept one can estimate maximum front inclination (inclination of compensation) by using the growth rate (7) as

$$\frac{\Delta X_{\max}}{D_0} = A\frac{u_w}{d_0}\tau_{comp}. \quad (8)$$

Perturbation compensation intensity is complicated function of local and global parameters of the system and cannot be determined analytically, nevertheless it may be estimated from qualitative physical considerations. Time of thermal reorganization of the system should be determined by some appropriate linear scale and velocity scales. Some upper estimate for τ_{comp} was proposed in [12] basing on system total length and thermal wave velocity (as velocity controlling system thermal reorganization) $\tau_{comp} \sim L/u_t$ which also leads to estimate for the maximum inclination amplitude $\Delta X_{\max} = u_w t_{comp} \sim Lu$. Note that the last estimate demonstrated reasonable correlation with experimental data [12].

The newer researches presented in this paper show that the system total length L is inadequate for τ_{comp} estimation. Combustor diameter D_0 and hot zone width H are reasonable scales controlling thermal compensation. Improving the physical analysis of the perturbation thermal compensation one should accept that velocity of the system thermal reorganization is $(u_t - u_w)$ (rather than u_t), as far as thermal wave propagation should be considered in the system of propagating FC wave. The principal correlation for τ_{comp} in this case has form

$$\tau_{comp} \sim \frac{D_0}{u_t - u_w} = \frac{D_0}{u_t(1-u)}. \quad (9)$$

Inclination of stabilization is expressed as follows

$$\frac{\Delta X_{\max}}{D_0} \cong B\frac{u}{1-u}\frac{D_0}{d_0}. \quad (10)$$

where B—empirical constant.

To develop concept of two stages of perturbation evolution considerable volume of reliable experimental data and numerical simulation is necessary. Below the experiments performed at elevated pressure in the system are described and results of 2D numerical simulation of the filtration combustion front perturbation dynamics are presented.

3. Experiment

Experiments were performed on facility, schematically presented on the Fig. 3. Burner was a quartz tube with inner diameter of 41 mm and wall thickness of 3 mm. Methane and air mixture was used as combustible. Gas flow rate and composition were controlled by rotameters with an accuracy of 5%. Compared to the experimental setup used in [12] a pressure control valve and pressure gauge were installed in the outlet pipeline. Tests were performed with a bed of Al_2O_3 balls with average diameter $d_0 = 3.5$ mm, porosity—0.4; Al_2O_3 heat capacity—1250 J/(kg K), density—1.7×10^3 kg/m^3. Ignition was made by spark plug placed into the bed. To improve ignition, large ceramic particles $d_0 = 7$ mm were placed in the area of electrodes (mixture failed to be ignited in the small balls). Ignition was performed at nearly stoicheometric mixture and after visible hot zone formation over complete cross-section, operation parameters were switched on. Filtration flow direction is taken for positive direction of the wave propagation. After front reached the last third of the burner, measurements were stopped.

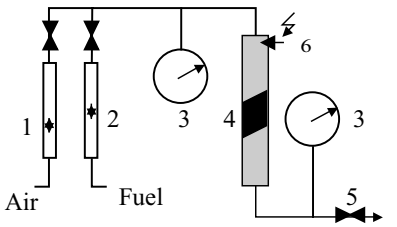

Fig. 3. Experimental set-up schematic diagram. 1, 2—flowmeters; 3—pressure gauge; 4—burner; 5—pressure control valve, 6—ignition spark plug.

Front "head" and front "tail" position was measured with optical cathetometer at fixed time intervals as an average result of several sequential measurements. Estimated accuracy of measurement being 15%. The front velocity u_w was defined as mean of the "head" and "tail" velocities. Dimensionless inclination of the front was defined as difference between the "head" and "tail" positions related to the tube diameter $\Delta X/D_0$. Average gas filtration velocity u_g was calculated regarding volumetric flow rate, tube cross-section and porosity. Thermal wave velocity was calculated according to definition $u_t = \langle (c_g\rho_g)/(c_s\rho_s)\rangle (m/(1-m))u_g$, where the brackets mean averaging by temperature interval $T_0 \ldots T_{\max}$, m—porosity. The average width of gasdynamic clog H was defined by formulae (5). The average by the cross-section combustion front temperature was evaluated as the mean one between adiabatic temperature of the FC wave $T_{ad}/(1-u)$ (with respect to wave propagation [8]) and temperature of the solid near the external boundary that was measured by pyrometer. The estimated accuracy of this assessment is 10%.

After ignition and reaching a steady state the visible wave front was perpendicular to filtration vector and had natural perturbations with the amplitude having the order of the bed grain size d_0. The characteristic time of hot zone width stabilization was ~3–4 min. After this time $T_{\max}$ and Δp were measured for H estimation and FC wave history was registered. The front moving, its

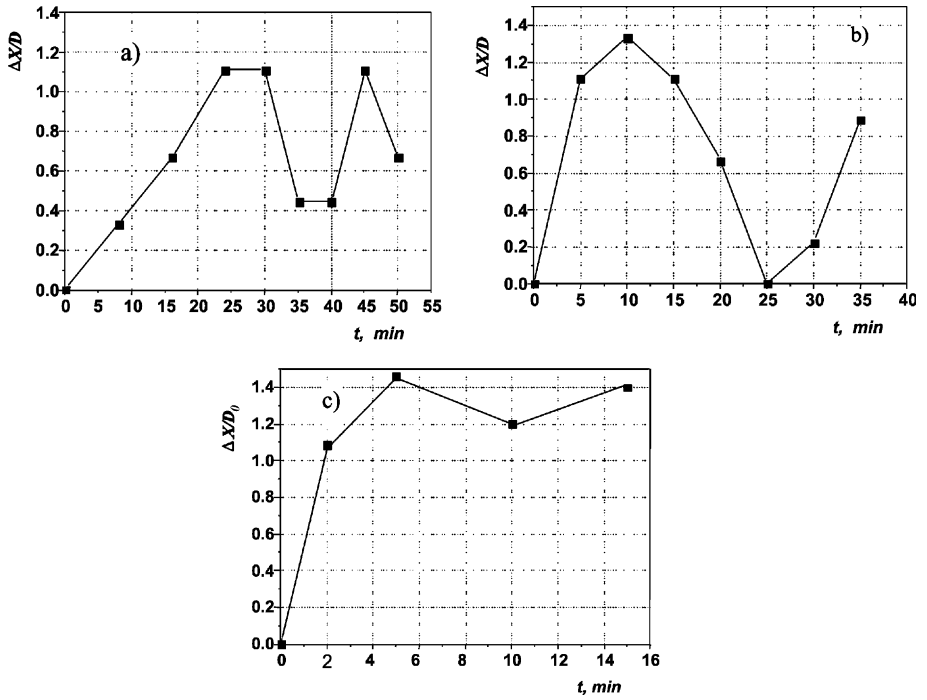

Fig. 4. Dynamics of Methane-air filtration combustion inclination. (a) $-F/A = 1/17$, (b) $-F/A = 1/18$, (c) $-F/A = 1/19$. $p = 1.5$ atm.

inclination grew and subsequently could stabilize or result in front break.

The measured dynamics of front inclination at 1.5 atm pressure is presented on the Fig. 4. The figure show that inclination amplitude grow approximately linearly at the beginning and rather quickly comes to saturation after that. We estimated linear speed of the amplitude growth $\partial\Delta X/\partial t = \Delta\dot{X}$ for the experiment runs and dimensionless $\Delta\dot{X}/u_w$ ratio. Taking into consideration the stohastic nature of perturbations one can conclude that average value of dimensionless amplitude growth speed to FC wave velocity ratio does not strongly depend on fuel, pressure and geometry of porous media and lays in interval from $\sim$1/4 to $\sim$1/2 with average value of $\sim$0.4.

In some cases experiments demonstrated regress of inclination amplitude after achievement of some maximum value and spiral movement of the front. This specific behavior was not observed in the earlier works and may be attributed to relatively low dimensionless velocity u and system thermal reorganization in time, particularly to growth of the hot zone width during wave propagation. The investigation of this specific behavior demands extensive experimental and 3D numerical study.

4. Numerical simulation and discussion

Multi-dimensional simulation may give precious information about front perturbation dynamics. Currently, 3D simulation straightened due to limited computational resources. Detailed 2D simulation is used for FC system simulation [13,14]. 2D simulation of front perturbation may be performed within plain symmetry of the system and is not completely adequate to the practical systems of cylindrical geometry. Nevertheless 2D simulation gives important data for qualitative investigation of perturbation dynamics.

2DBurner software package [13] was used for numerical simulation of the FC front perturbation evolution. The basic equations defining the gas mixture dynamics were the equations of state $\rho_g = pM/RT_g$, continuity $\nabla(\rho_g \mathbf{u}_g) = 0$, and filtration equation $-\nabla p = \frac{\mu}{k}\mathbf{u}_g + \frac{\rho_g}{k}|\mathbf{u}_g|\mathbf{u}_g$. Model includes energy and mass conservation for each mixture component expressed by equations:

$$c_p\rho_g\frac{\partial T_g}{\partial t} + c_p\nabla(\rho_g\mathbf{u}_g T_g) - \nabla(\mathbf{\Lambda}\otimes\nabla T_g) = \frac{\alpha_{vol}}{m}(T_s - T_g) - \sum_i h_i\dot{\rho}_i,$$

$$(1-m)c_s\rho_s\frac{\partial T_s}{\partial t} - \nabla(\lambda_s\nabla T_s) = \alpha_{vol}(T_g - T_s),$$

$$\rho_g\frac{\partial c_i}{\partial t} + \nabla(\rho_g\mathbf{u}_g c_i) - \nabla(D\otimes\nabla c_i) = \dot{\rho}_i. \quad (11)$$

Here h_i—specific enthalpy of ith component, $\dot{\rho}_i$—mass generation of ith component due to chemical reactions, $(\sum_i \dot{\rho}_i = 0)$; $\mathbf{D} = D_g\mathbf{I} + \mathbf{D}_d$, where $\mathbf{D}_d$ is a dispersion

diffusion tensor, $\mathbf{\Lambda}$—dispersion heat conductivity tensor defined similarly to $\mathbf{D}$ [8,15].

Grey body irradiation at inlet, outlet cross-section and burner sides is assumed

$$-\lambda\frac{\partial T_s}{\partial z}=\varepsilon^*_{ext}\sigma(T_s^4-T_0^4). \tag{12}$$

The following primary parameters were accepted for the standard case: effective heat conductivity in the carcass:

$$\lambda=\lambda_s+\frac{16}{3}\left(\frac{0.666m}{1-m}+0.5\right)d_0\varepsilon^*_{int}\sigma T_s^3; \tag{13}$$

volumetric heat exchange coefficient [15]:

$$\alpha_{vol}=\frac{\lambda_g 6(1-m)}{d_0^2}\left[2+1.1\,\mathrm{Pr}^{1/3}\left(\frac{m\rho_g u_g d_0}{\mu}\right)^{0.6}\right]; \tag{14}$$

permeabilities [8]: $k=(d_0^2m^3/150(1-m)^2)$, $\tilde{k}=(d_0m^3/1.75(1-m))$. Nitrogen diffusion, viscosity and heat conduction coefficients were used for gas mixture. The following approximations with characteristic accuracy 5% in all temperature range were utilized: $D_g=0.18((T/273))^{1.75}$ (p_0/p) cm^2/s; $p_0=1.013\times10^5$ Pa; $\lambda_g=1.4\times10^{-2}+4.8\times10^{-5}\times T$, W/(m K); $\mu=4.4\times10^{-7}\times T^{0.65}$ Pa s. The second order methane oxidation brutto-kinetics [13] $\mathrm{d}[CH_4]/\mathrm{d}t=-3.6\times10^{-10}[CH_4][O_2]\exp(-15640/T)$ was used (concentrations $[CH_4]$ and $[O_2]$ have dimension cm^{-3}). Other parameters accepted for the standard case are as follows: solid emissivity $\varepsilon^*_{ext}=0.4$, $\varepsilon^*_{int}=0.4$; tube length $L=0.4$ m; plain burner width $D_0=0.038$ m; outlet pressure, $p_0=1.013\times10^5$ Pa, porosity $m=0.4$; gas molecular weight $M=0.029$ kg/mol; bedding particle diameter $d_0=0.004$ m; methane heat content $H=5.3$ e7 J/kg; porous media heat conduction coefficient $\lambda_s=0.2$ J/(m K); volumetric flow rates of methane and air mixture was $G=100$ m^3/(h m), concentration of methane at inlet is 4%, concentration of oxygen in air—0.21, longitudinal and transverse dispersion diffusivity $D_p=0.5d_0u_g$, $D_t=0.1d_0u_g$.

The perturbation was introduced in the system as an inclination with amplitude equal to particle diameter. The startup and intermediary temperature distribution for the standard case is presented in the Fig. 5.

Parameters that were varied during numerical investigation of inclination dynamics are divided into three groups and presented in the Table 1.

To investigate the influence of the system parameters on the perturbation evolution the correspondent dynamics curves were simulated and compared with each other graphically, Figs. 6–13. The filtration combustion wave velocities for unperturbed front were obtained numerically for all simulation cases (Table 2) and used to check theoretical dependences (7), (10). Note, that wave propagation is not strictly steady state process and characteristic accuracy of the presented in the Table 2 parameters ~3–5%.

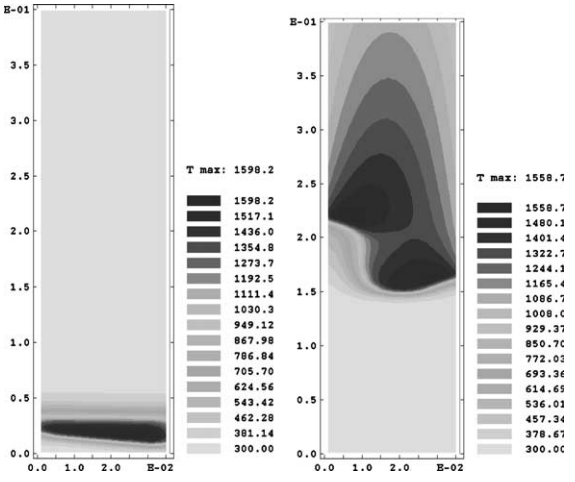

Fig. 5. Simulated 2D temperature fields of filtration combustion wave at startup and intermediary time moment. CH_4 concentration in air mixture 4%. $p=1.5$ atm.

Table 1
Set of the FC system parameters utilized for perturbation dynamics parametric study

Group of parameters	Parameter	Variable notation
Parameters, controlling internal heat transfer in the system	• Filtration velocity	u_g
	• Adiabatic combustion temperature (mixture heat content)	T_{ad}
	• Diameter of the bedding particle	d_0
	• System pressure	p_o
Parameters of geometry of the burner	• Burner length	L
	• Burner diameter	D_0
Parameters of boundary and initial thermal conditions	• Coefficient of Newtonian heat losses	β_o
	• Ignition preheating zone width	H_0

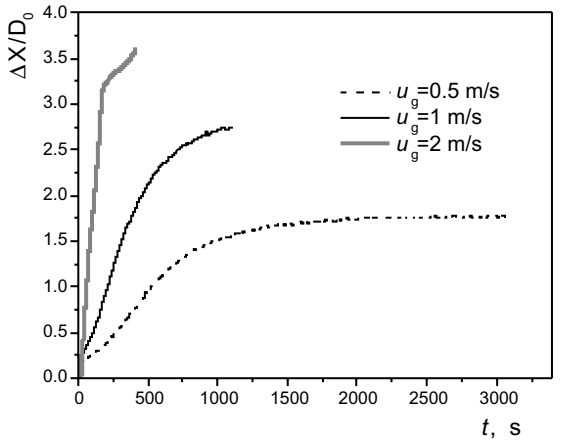

Fig. 6. Front inclination dynamics for different gas filtration velocities.

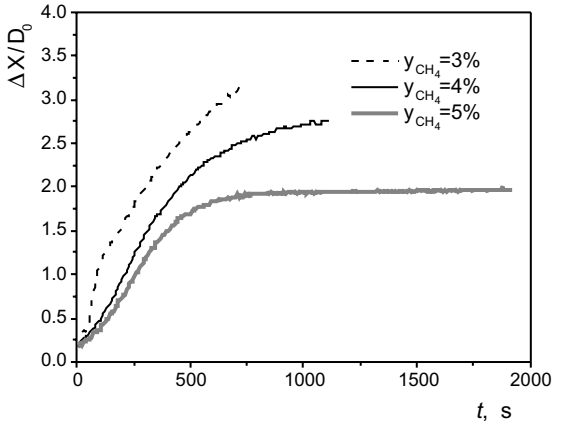

Fig. 7. Front inclination dynamics for the mixtures with different calorific contents.

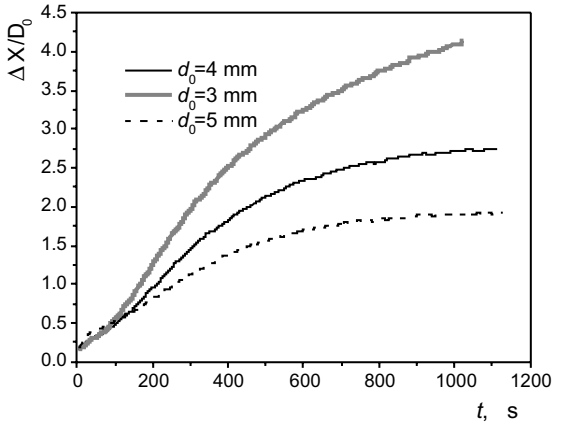

Fig. 8. Front inclination dynamics for porous media pickings with different particle size.

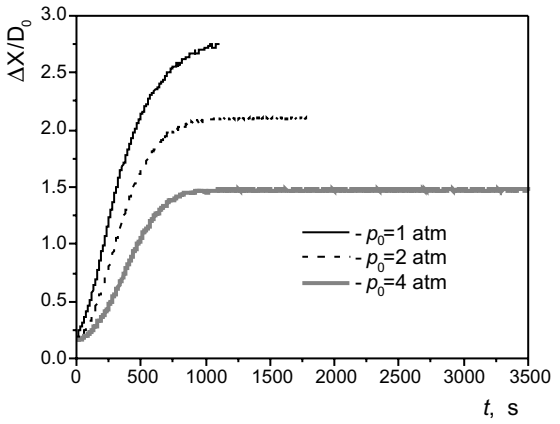

Fig. 9. Front inclination dynamics for the systems with different pressure.

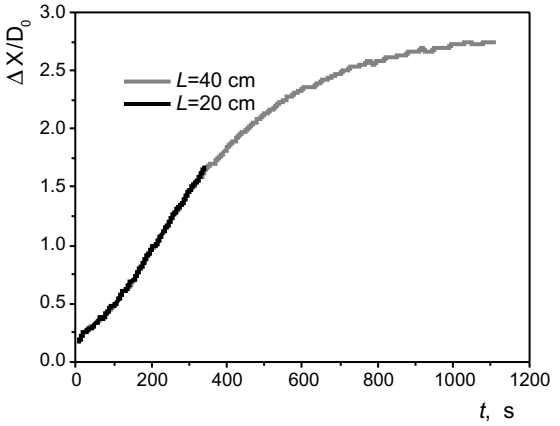

Fig. 10. Front inclination dynamics for the systems with different total porous media length.

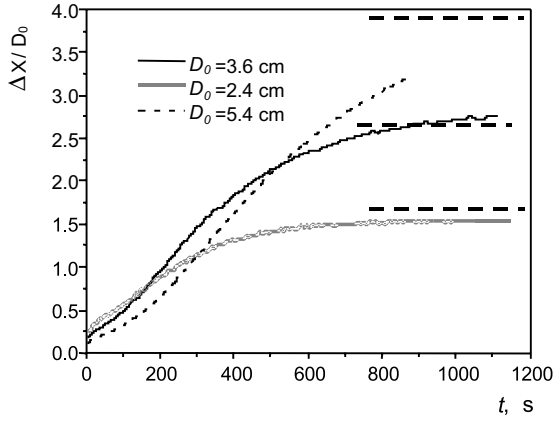

Fig. 11. Front inclination dynamics for the systems with different burner diameter.

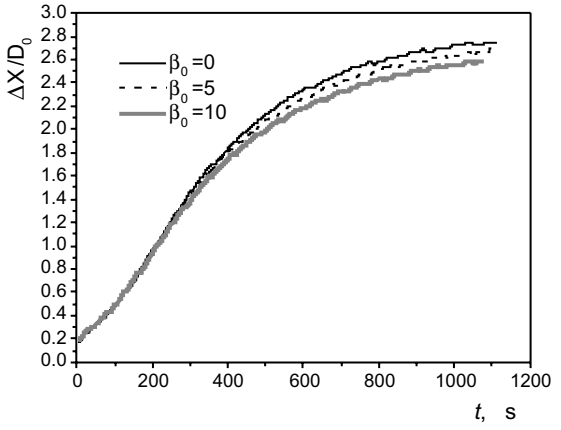

Fig. 12. Front inclination dynamics for the systems with different side thermal losses.

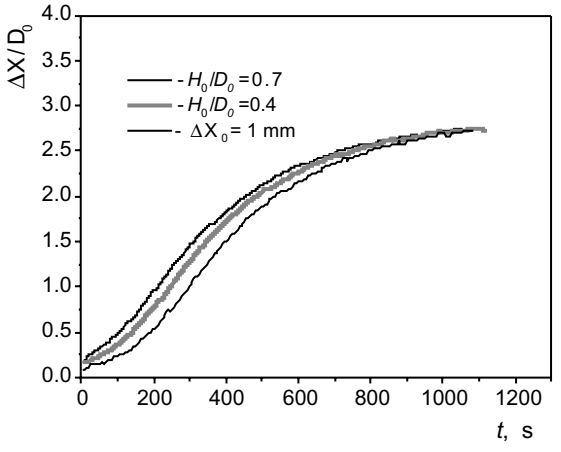

Fig. 13. Front inclination dynamics for the systems with different startup preheating zone width H_0/D_0 and reduced startup front inclination ΔX_0.

Three phases are clearly distinguished on all numerically obtained curves. That are: startup transient phase, linear growth and perturbation compensation phases. The first phase is short in time (~100 s) and physically conditioned by establishment of FC wave profile after combustion ignition. Another two phases are system conditioned perturbation evolution.

The front inclination dynamics for different gas mixture filtration velocities (or flow rates) is presented on the Fig. 6. Comparison of the dynamic curves demonstrates linear correlation between inclination growth rate $\Delta\dot{X}/D_0$ and wave velocity u_w as well as with filtration flow rate and thermal wave propagation velocity u_t. Nevertheless correlation with u_w is more accurate (proportionality constant is close to unity). The inclination saturation amplitude is not proportional to u_w as far as perturbation compensation processes starts some earlier in the case of higher flow rate (being checked by dynamic curve twist point on the graph). It is easy to see (by using data of the Table 2) that expected according to (10) correlation with $u/(1-u)$ is more accurate than proposed earlier [12] proportionality to u.

The influence of the fuel mixture heat content on the inclination dynamics is demonstrated in the next series of simulation (Fig. 7). The concentrations of methane $y_{CH_4} = 3\%$, 4% and 5% in the air correspond to adiabatic temperature increase $\Delta T_{ad} \cong 746$, 968, 1173 K correspondently. One can see that inclination growth rate $\Delta\dot{X}/D_0$ is proportional both to u_w and dimensionless wave velocity u and inversely proportional to mixture heat content and adiabatic temperature. Similar correlations take place for the inclination saturation amplitude as far as perturbation compensation starts simultaneously for all cases.

The results of perturbation dynamics simulation in the burner with for different particle size are presented on the Fig. 8. It is easy to see that inclination growth rate correlates directly with u_w and inversely with particle diameters. The complex u_w/d_0 corresponding to

Table 2
Calculated characteristics of the unperturbed FC wave

No.	Case description	$u_w \times 10^4$ m/s	$u_t \times 10^4$ m/s	u	$u/(1-u)$	T_{max}, K
1	Standard case	3.04	8.36	0.364	0.572	1678
2	Reduced flow rate ($u_g = 0.5$ m/s)	1.26	4.13	0.304	0.436	1561
3	Increased flow rate ($u_g = 2$ m/s)	6.79	16.7	0.407	0.686	1756
4	Reduced heat content ($y_{CH_4} = 3\%$)	4.04	8.22	0.491	0.965	1584
5	Increased heat content ($y_{CH_4} = 5\%$)	2.17	8.42	0.257	0.346	1760
6	Reduced particles size ($d_0 = 3$ mm)	3.14	8.39	0.374	0.597	1701
7	Increased particles size ($d_0 = 5$ mm)	2.97	8.29	0.358	0.558	1655
8	Reduced pressure ($p_o = 0.5$ atm)	3.83	8.55	0.447	0.808	1842
9	Increased perssure ($p_o = 2$ atm)	2.18	8.14	0.268	0.366	1520
10	Increased pressure ($p_o = 4$ atm)	1.25	8.07	0.155	0.183	1388
11	Increased heat losses ($\beta = 5$)	3.12	8.35	0.374	0.597	1670
12	Increased heat losses ($\beta = 10$)	3.19	8.34	0.383	0.621	1662

formula (7) gives best correlation with initial (linear) growth rate (the corresponding value for this complex: 0.59, 0.76 and 1.05). This peculiarity evidences that the structure of the front (particularly preheating zone width) influence considerably perturbation dynamics. Note that particle size d_0 is introduced into SP analysis via front preheating zone width only.

In Fig. 9 the inclination dynamics graphs for the cases of different pressure are presented. One can observe considerable influence of pressure on inclination dynamics. In the considered cases the correlation $\Delta\dot{X}/D_0 \sim u_w$ prevails although the coefficient of proportionality is less than unity. This may be explained by pressure influences on the width of the filtration combustion front.

In Fig. 10 the inclination dynamics graphs obtained for different system lengths are presented. One can see that front dynamics is identical for both cases at least at linear stage and in the beginning of the non-linear compensation stage. The independence of the perturbation growth rate of system length (as well as the global parameters) on linear stage complies with theoretical estimation (7). Identical perturbation evolution on the stage of compensation let one conclude of negligible influence of total combustor length L on the perturbation compensation. Consequently, the appropriate length scales for perturbation compensation time estimates are system diameter D_0 and hot zone width H.

Variation of another macroscopic parameter—burner diameter leads to non-trivial, from the first sight, behavior of perturbation dynamics curves (Fig. 11). Examination of graphs let one conclude that dynamics curves differ by duration of the startup transient phase which is explained by different initial conditions for these cases. The inclination growth rates on the linear growth stage are close for all three cases and consequently, system diameter D_0 does not influence dimensionless inclination rate on the linear stage. (Note that value of u_w for unperturbed front are the same for all three cases). Simulation shows that system perturbation compensation is more intensive in the cases of smaller diameter, which results in smaller saturation amplitude of inclination. The proportionality for the inclination compensation time $\tau_{comp} \sim D_0$ may be accepted. Numerical simulation let us recommend numerical coefficient $B = 0.5$ in the theoretical estimate (10). The corresponding inclination amplitudes are marked by horizontal dot lines on the Fig. 11.

The influence of the system side losses was examined by calculation of the front inclination dynamics, side losses coefficient β being varied. Visual analysis of the graphs Fig. 12 let one conclude of weak influence of conditions of external heat exchange on front dynamics on initial (linear) stage. At the later non-linear stage simulation show some faster perturbation compensation for the case of higher side losses. This is an unexpected result as far as dimensionless wave velocity u is slightly higher in the case of heat losses. At the same time this result evidences of existence of a mechanism accelerating perturbation compensation due to side losses. One should also keep in mind inaccuracy introduced by plain symmetry of the simulated system.

Another set of numerical simulations was performed to investigate the influence of initial conditions on inclination dynamics. The following parameters, defining initial conditions were used: width of initially preheated (startup) zone, the temperature of the initially preheated zone and initial (startup) amplitude of front inclination. Numerical experiments show that startup parameters influence the front geometry only on the startup transient stage and have no considerable influence on the linear growth stage and following perturbation evolution. Inclination dynamics for the different startup preheating zone widths is presented on the Fig. 13. One can see that dynamics curves are similar except of some time delay shift.

5. Conclusion

The presented materials should be considered as development and generalization of the earlier results [12]. The paper introduce the modern physical concepts of complicated phenomena—filtration combustion front perturbation evolution. New experiments and 2D numerical simulation gives all grounds to assert of filtration combustion systems property to compensate front perturbations via thermal reorganization. Numerical modeling shows that three phases of perturbation evolution may be distinguished: startup transient phase, linear growth and perturbation compensation phases.

Parametric dependences of inclination growth rate at the linear stage are specified. The main correlations following from SP analysis are confirmed by numerical and experimental study. It is shown that the porous media particle size d_0 influences the inclination growth rate via correlation with front width (6). The inclination amplitude growth rate at the linear stage determined by local FC front parameters:

$$\Delta\dot{X}/D_0 = A \cdot u_w/d_0.$$

For inert packings and gaseous hydrocarbon fuels constant $A \approx 0.04$ according to experiments.

Inclination dynamics on the non-linear stage is determined by intensity of perturbation compensation. It can be characterized by characteristic time τ_{comp} and thus determine maximum inclination (inclination of compensation)

$$\frac{\Delta X_{max}}{D_0} = A\frac{u_w}{d_0}\tau_{comp}.$$

Perturbation compensation intensity is complicated function of local and global parameters of the system and cannot be determined analytically. Nevertheless it may be estimated as ratio of characteristic length and velocity scales. It is found that combustor diameter D_0 and hot zone width H may be used as characteristic length controlling thermal compensation. Usage of the system total length L is inadequate.

It is shown that characteristic velocity of the system thermal reorganization is better described by $(u_t - u_w)$, as far as thermal weave propagation should be considered in the system of propagating FC wave. The principal correlation for τ_{comp} in this case:

$$\tau_{comp} \sim \frac{D_0}{u_t - u_w} = \frac{D_0}{u_t(1-u)}.$$

According to the above equations inclination of stabilization is expressed as follows

$$\frac{\Delta X_{max}}{D_0} = B\frac{u}{1-u}\frac{D_0}{d_0}, \tag{15}$$

where value $B = 0.5$ may be recommended for empirical constant.

Some physical factors potentially influencing the perturbation dynamics: front mean temperature decrease at inclination growth; multi-dimensional character of the front and boundary effects should be examined in more detail. Except of quantitative characteristics, having practical interest, some fundamental problems deserve attention. One of the problems is capability of the perturbed front to evolve to its normal orientation (or stability of the perturbed to saturation front configurations). Another interesting problem is conditions and properties of spinal front propagation regime.

Numerical simulation is found to be effective for more accurate description of perturbation dynamics. New results in this direction are expected by using 3D simulation codes.

Acknowledgement

This research was sponsored by Fondecyt grant # 7010354.

References

[1] Yu.Sh. Matros, Heat Wave Propagation in Heterogeneous Media (in Russian), Nauka Publishers, Novosibirsk, 1988.
[2] J.R. Howell, M.J. Hall, J.L. Ellzey, Combustion of hydrocarbon fuels within porous inert media, Prog. Energy Comb. Sci. 22 (1996) 122–145.
[3] L.A. Kennedy, A.A. Fridmanand, A.V. Saveliev, Superadiabatic combustion in porous media: Wave propagation, instabilities, New type of chemical reactor, J. Fluid Mech. Res. 22 (1996) 1–26.
[4] S.S. Minaev, S.I. Potytnyakov, V.A. Babkin, Combustion wave instability in the filtration combustion of gases, Combust., Explo. Shock Waves 30 (1994) 306–310.
[5] P.V. Vainstein, Gas flame stability in porous media, Combust., Explo. Shock Waves 28 (1992) 28–34.
[6] N.A. Kakutkina, V.S. Babkin, Characteristics of stationary spherical waves of gas combustion in inert porous media, Combust., Explo. Shock Waves 34 (1998) 150–159.
[7] Chemical Physics Technologies Co. Report on R&D Services Agreement from January 1 1996, Part 1. Minsk, Heat and mass transfer Institute, 1996.
[8] K.V. Dobrego, S.A. Zhdanok, Physics of filtration combustion of gases, Heat and mass transfer Institute Publ, Minsk, 2002 (in Russian).
[9] K.V. Dobrego, S.A. Zhdanok, A.V. Krauklis, E.I. Khanevich, A.I. Zaruba, Investigation of the filtration combustion stability in cylinder porous body radiative burner, J. Eng. Phys. Thermophys. 72 (1999) 599–605.
[10] S.A. Zhdanok, K.V. Dobrego, Theory of thermohydrodynamic instability of the front of filtration combustion of gases, Combust., Explo. Shock Waves 35 (1999) 476–482.
[11] V. Bubnovich, C. Rosas, K. Dobrego, S. Zhdanok, Analisis de la inestabilidad termica e hidrodinamica del frente de combustion del gas en medios porosos, Proceedings of IV Congreso Iberoamericano Dce Ingenieria Mecanica, 23–26 November 1999, Santiago, Chile, 1999.
[12] K.V. Dobrego, S.A. Zhdanok, A.I. Zaruba, Experimental and analytical investigation of the gas filtration combustion inclination instability, Int. J. Heat Mass Transfer 44 (2001) 2127–2136.
[13] K.V. Dobrego, I.M. Kozlov, S.A. Zhdanok, N.N. Gnezdilov, Modeling of diffusion filtration combustion radiative burner, Int. J. Heat Mass Transfer 44 (2001) 3265–3272.
[14] S.I. Shabunia, V.V. Martynenko, 2D modeling of filtration combustion in inert porous media in one-temperature approximation, J. Eng. Phys. Thermophys. 71 (6) (1998) 963–970.
[15] N. Wakao, S. Kaguie, Heat and Mass Transfer in Packed Beds, Gordon and Breach Science Publishers, 1982.